J Mater Sci: Mater Med (2008) 19:1981–1990
DOI 10.1007/s10856-007-3283-3

Structural heterogeneity of pharmaceutical compacts probed by micro-indentation

Jonghwi Lee

Received: 18 June 2007 / Accepted: 18 September 2007 / Published online: 18 October 2007

Abstract Indentation has been used for several decades to conveniently assess the hardness and modulus of various compacts. However, this measurement is dependent on the size of the indentation area from a few nanometers to several millimeters, which is determined by the maximum indentation force (MIF). Micro-indentation often loses its ability to give an accurate representation of the hardness due to its relatively small micron-size indentation area compared with the dimensions of the structural inhomogeneity of compacts. This study used a different approach to micro-indentation by examining whether this method can probe the inhomogeneity of compacts with varying MIF. Two typical pharmaceutical excipients, one brittle and one ductile, were used as model compacts. The representative hardness and modulus values were available when the MIF was >1000 mN. Changes in the standard deviation of the indentation hardness reflected the structural inhomogeneity of the compacts, which was found to increase with decreasing MIF to below 800 mN in the case of the microcrystalline cellulose compacts. The information on the structural inhomogeneity obtained by micro-indentation appears to be consistent with the observations from microscopy investigations. Anisotropy and other related structural information could be readily obtained by probing the two different surfaces of compacts with changing MIF, one parallel and the other perpendicular to the compaction pressure direction.

J. Lee (✉)
Department of Chemical Engineering and Materials Science, Chung-Ang University, 221 Heukseok-dong, Dongjak-gu, Seoul 156-756, South Korea
e-mail: jong@cau.ac.kr

1 Introduction

Hardness tests have been widely used in the pharmaceutical industry to examine solid dosage forms since the 1970's [1–8]. Ironically, the meaning of hardness is often used inappropriately. The strength of tablets in common compression tests is often called 'hardness'. However, the actual definition of hardness is a material's resistance against plastic deformation [1, 9]. The compression strength and indentation hardness have different stress states with the former being related to the final failure properties and the latter to the initial deformation of materials.

Indentation is a simple test that can provide the elastic, plastic, and viscoelastic information of materials. In particular, the indentation hardness and the modulus of tablets can be measured simultaneously. The indentation hardness is a useful property that is related to many other parameters for compaction and disintegration [10–13]. Indentation does not require a large volume of materials or difficult sample preparation. Furthermore, this test is more useful because the compressive stress state generated by indentation is similar to what the tablets and powders experience during pharmaceutical unit operations [10, 14].

According to the Leuenberger equation for the Brinell hardness, in a typical indentation test of a compact, the hardness (H), relative density (ρ), and compaction pressure (σ) are interrelated as follows: $H = H_{max}(1 - e^{-\chi\sigma\rho})$ where H_{max} is the maximum hardness (compactibility), and χ is the pressure susceptibility (compressibility) [1]. The Heckel method uses a slightly different equation for the Vickers hardness as follows [1]: $\ln(1–H/H_{max}) = \chi\sigma\rho$. In both equations, the compacts were assumed to be

homogeneous [1]. In order to make the assumption reasonable, the size of the indenter (or probing area) should be sufficiently larger than the size of the particles constituting a compact.

Indentation can be classified according to the load range of the indenter, i.e., macro-, micro-, and nano-indentation. When the indentation force is <10 N, it is known as micro-indentation [1]. Micro-indentation tests typically probe an area ranging from 5 to 500 μm^2 (ca. 100–7,000 mN).

In an ideal case, the mechanical properties of the whole compact can be represented by the modulus, hardness, and fracture toughness of a small volume probed by an indenter [7]. Conventional tests generally use macro- and sometimes micro-indenters to obtain representative values. On the other hand, nano- and micro-indentation have been used to characterize single particles e.g. a single crystal of a drug [2–4, 6, 12, 13, 15–19]. Crystallization processes resulting in different crystal structures were monitored successfully using this nano-indentation technique [11, 12].

The face of single crystals (a well-defined surface) is ideal for indentation tests. However, for pharmaceutical compacts, the structural inhomogeneity that inevitably exists complicates micro-indentation analysis. Although micro-indentation tests are still convenient and require a relatively small amount of sample, they are seldom used for fundamental research due to their difficulty in interpretation [5].

Only a few studies on non-pharmaceutical materials have considered the inhomogeneity of materials. The inhomogeneity according to the depth of the indentation was monitored by measuring indentation hardness values as a function of the indentation depth [20]. Investigation on the inhomogeneity-related issues in the micro-indentation tests of pharmaceutical compacts has never been reported to the best of our knowledge.

This study examined what types of valid interpretations can be obtained from micro-indentation tests on pharmaceutical compacts besides conventional indentation hardness, modulus, and fracture toughness values. The main focus was on how to identify or interpret the influence of structural inhomogeneity. Compacts of a ductile (microcrystalline cellulose) and brittle (lactose monohydrate) material were used. After compaction, the primary particles turn into the grains of the compacts and serve as a potential cause of the structural inhomogeneity. The size of the primary particles is usually within the probing area range of micro-indentation. The micro-indentation results were correlated with the scanning electron microscopy (SEM) and atomic force microscopy (AFM) images.

2 Materials and methods

2.1 Materials

Lactose monohydrate fast flo (LT, Foremost) and microcrystalline cellulose (MC, FMC, Avicel PH101) were used as received. Compacts of two geometries, 8 × 4.5 mm rectangular plate and 10.3 mm disk (face dimensions), were prepared using a Carver Press (model 3850). The thickness varied according to compaction force and sample weight. The compaction force was applied for 10 s, and unless otherwise specified, the compaction force was 4,000 kgf. The weights of the samples were 20 and 100 mg for the two geometries, respectively. All the indentation tests were performed at least 24 h after compaction.

2.2 Micro-indentation and other characterizations

A micro-indentation tester (CSEM Instruments Micro Hardness Tester, 30–30,000 mN) was used with a Vickers hardness tip at room temperature (relative humidity = 40–54%). The Vickers diamond tip has an 136° angle between the adjacent faces and a 68° angle between any of the four facets and the vertical direction of the applied load. Unless mentioned otherwise, the loading rate was 1,000 mN/min, and the center parts of the compacts were tested. (Based on initial investigations, the loading rate was chosen.) Each indentation hardness or modulus value was an average from at least nine repeated tests (three specimens). The tester-related mechanical artifacts were reduced by inserting a pause of 10 sec between the loading and unloading steps.

The Oliver and Pharr method was used to calculate the hardness and modulus values under the hypothesis that the poisson ratio was 0.3 [21, 22]. The upper 80% of the unloading data was used to fit the power law of the Oliver and Pharr method (geometric constant ε was assumed to be 2).

The environmental scanning electron microscopy (ESEM) results were obtained using an ElectroScan Model 2,010 at 5 Torr and 15 kV. The tapping mode AFM images were obtained using a Digital Instruments Dimension™ 3100 and TESP or TESP7 etched single crystal silicone probes (20–100 N/m force constant and 200–400 kHz resonance frequency) under ambient conditions.

3 Results

3.1 General indentation curves

Micro-indentation produces force data as a function of the indentation depth. Figure 1 shows a typical

loading-unloading curve with a schematic illustration of the indentation volume and inhomogeneous compact structure. As shown in the curve, the indentation process is not perfectly elastic. There is significant hysteresis between the loading and unloading curves. The hysteresis indicates the energy dissipated by the indentation volume. The area under the unloading curve is the elastic work on recovery [1].

The unique point of *micro*-indentation is that the size of the indenter is close to the 'wavelength' of the spatial fluctuation of the mechanical properties [inhomogeneity of compacts (The 'wavelength' concept is used similar to that in the density fluctuation of condensed matter.)]. Figure 1 gives a schematic illustration of the simplified granular structure, which indicates the inhomogeneous characters of the compacts. There are always mechanically strong and weak regions in a compact. For example, the particle boundaries or internal cracks will be mechanically weaker than the single crystal regions. The fluctuation in the mechanical properties could be in the micron or nanometer range. Representative values of the mechanical properties can be obtained by averaging the results of multiple micro-indentations covering a sufficiently large surface area, while they can readily be available from a *macro*-indentation test.

Figure 1 shows four different indentation volumes. As the size decreases well below the 'wavelength' of structural inhomogeneity, the relative position of an indenter and a mechanically weak (or strong) region determines the resulting hardness of that position. Hence, the standard deviation in the hardness results is dependent on the indenter size. On the other hand, an average hardness value would remain constant regardless of the indentation volume if a large number of indentation tests are performed and no other complications such as the 'strain gradient' effect [23, 24] are considered.

3.2 Inhomogeneity probed by indentation hardness

The indentation hardness of MC was found to increase with decreasing maximum indentation force (MIF), as shown in Fig. 2. This increase has been widely observed in most indentation experiments, which will be discussed later. The indentation modulus always shows the same trend as indentation hardness (Fig. 2). Therefore, the modulus data is not presented in this report even though the same structural investigation can be performed using modulus data.

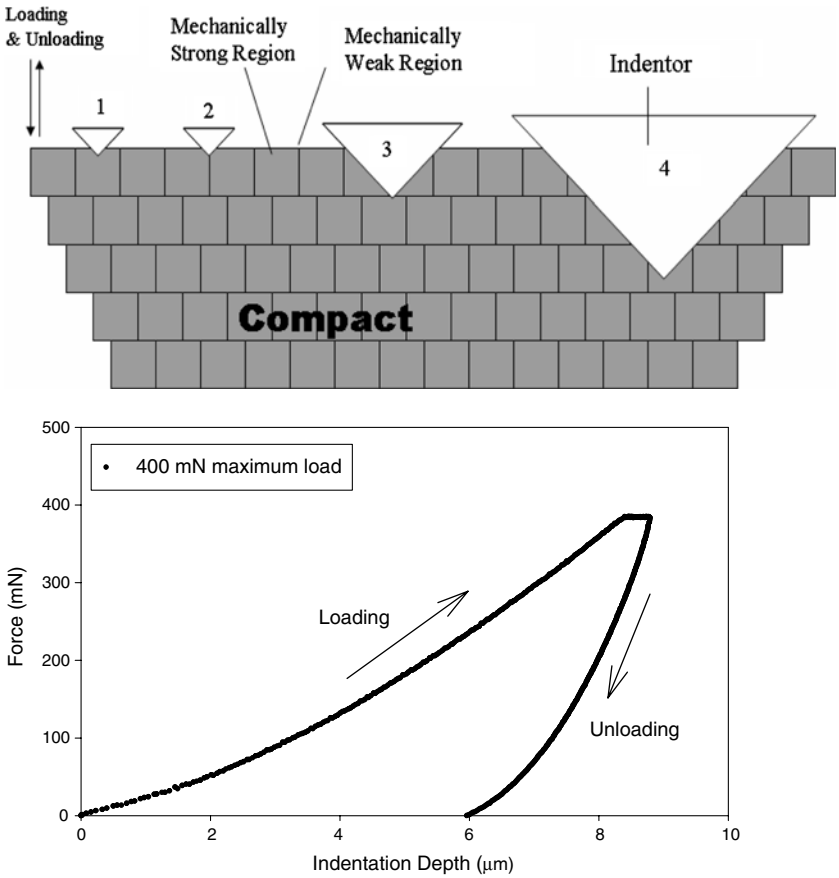

Fig. 1 Schematic illustration of micro-indentation volume and inhomogeneous compact structure (upper) and typical force-indentation depth (load-displacement) curve obtained (lower). Four indenters were drawn to demonstrate their size effect relative to the inhomogeneity of compact

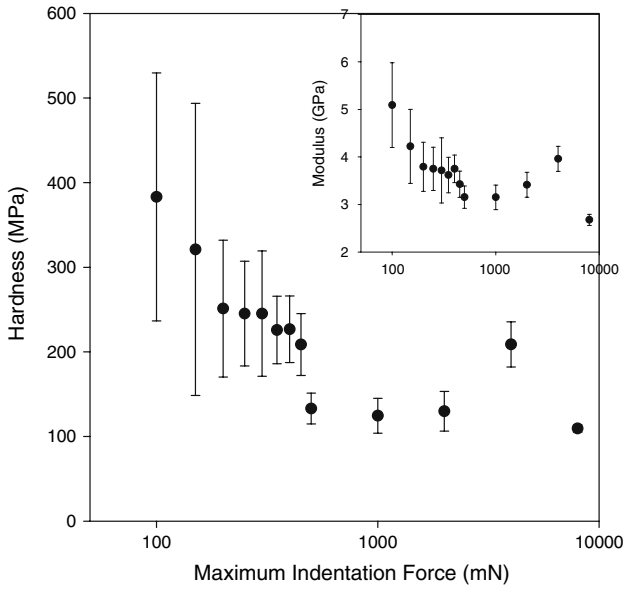

Fig. 2 Indentation hardness and modulus (inlet) of microcrystalline cellulose compacts as a function of maximum force of indentation (rectangular plate samples)

In Fig. 2, the standard deviation of both the indentation hardness and modulus was found to increase with decreasing MIF. Figure 3 shows a plot of the standard deviation versus MIF. The plot shows an increase in the standard deviation at 800 mN, which can also be found in the plot of the modulus versus the MIF (inlet). It is possible that these values are representative of the average hardness of the compacts considering the consistent hardness values with the relatively small standard deviation at a MIF >1,000 mN.

The standard deviation increases as the MIF decreases to <800 mN, which might mean that the indentation volume becomes close to or below the size of the inhomogeneity of the compacts (Figs. 1 and 3). Although the size of the inhomogeneity is not well defined, the essential aspects of the influence of inhomogeneity expected in Fig. 1 appear to be true for actual compacts with complicated inhomogeneity.

Figure 4 shows the changes in the standard deviation of the LT compacts prepared under two different pressures. A decrease in the MIF triggers an increase in the standard deviation in both curves. Compared with the MC case in Fig. 2, the increase appears to be rather smooth. The increases in the standard deviations of the MC and LT began when the contact areas (A_c) had diameters of 20 and 40 μm, respectively.

When the compaction pressure was 409 MPa, the standard deviation appeared to increase not only with decreasing MIF but also with increasing MIF above 1,200 mN. An increase in standard deviation with increasing MIF above 1,200 mN was seldom found as will be found in Fig. 7. This might be related to compaction-induced defects such as surface cracks caused by the brittle nature of the materials. LT is usually considered to be more brittle than MC [10].

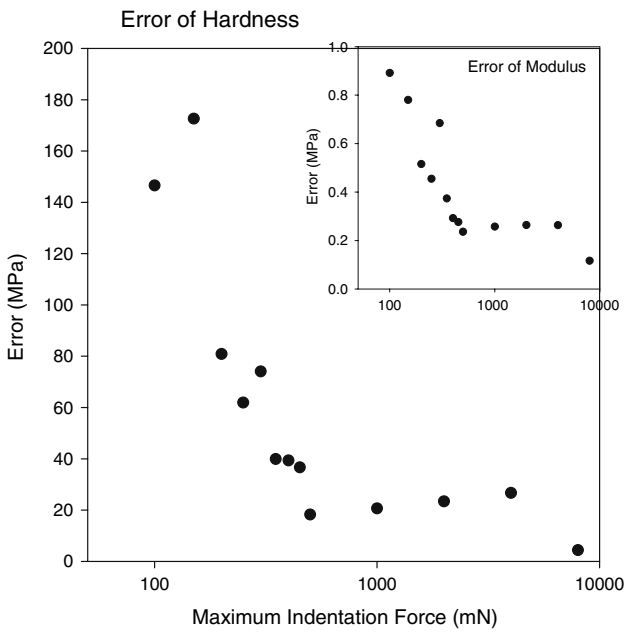

Fig. 3 Standard deviations of indentation hardness and modulus (inlet) plotted in Fig. 2 as a function of maximum force of indentation (rectangular plate samples)

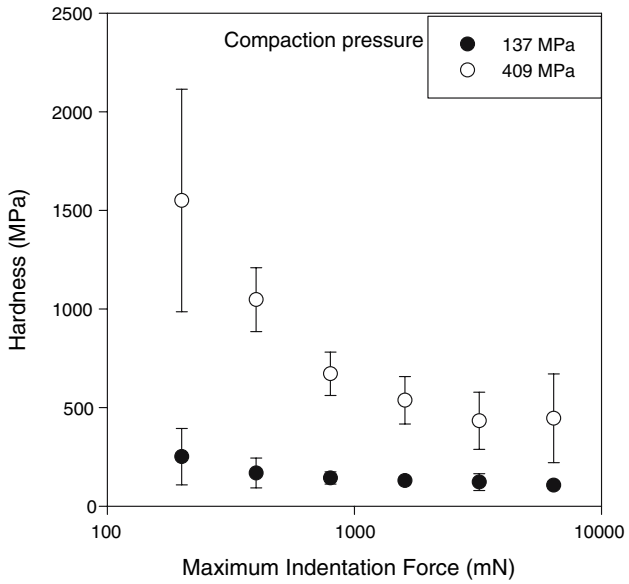

Fig. 4 Indentation hardness of lactose compacts as a function of maximum indentation force. (rectangular plate samples) (**a**) Microcrystalline cellulose, particles (**b**) Lactose, particles (**c**) Microcrystalline cellulose, 400 mN (**d**) Microcrystalline cellulose, 4,000 mN

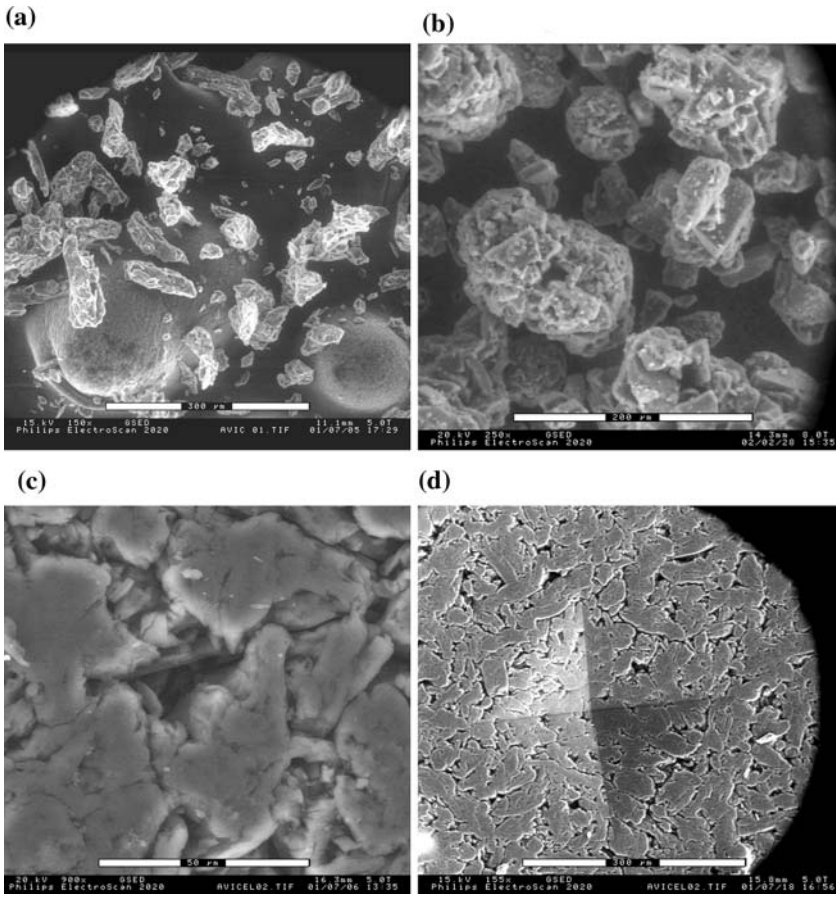

Fig. 5 ESEM micrographs: (**a**) microcrystalline cellulose particles; (**b**) lactose particles; (**c**) indent on a microcrystalline cellulose compact produced by 400 mN MIF; (**d**) indent on a microcrystalline cellulose compact produced by 4,000 mN MIF. (rectangular plate samples)

3.3 ESEM investigation of indents

SEM and AFM can be used to trace the actual structural inhomogeneity. Fig. 5a and b shows the particles before compaction. Their sizes ranged from 50 to 100 μm. After compaction, the interfaces between the primary particles served as the sources of mechanically weak regions. Voids can exist between the primary particles, whose volume fraction is directly related to the compaction pressure. Therefore, the shape and size of the primary particles might be important in determining the homogeneity of the mechanical properties in a compact. Indeed, the grain structure of the compacts (Fig. 5c and d) reflects the primary particle shape of the MC particles, and there are significant micro-voids (microcracks) between grains.

Figure 5c and d show the indents on the surface. When the MIF was 400 mN, the size of the indent was comparable to or smaller than the grain size, resulting in a relatively large standard deviation in the micro-indentation data (Fig. 3). The indent in Fig. 5c appears to form near an interface region not in the middle of a grain, possibly resulting in a relatively smaller hardness value. When the MIF was 4,000 mN (Fig. 5d), the indentation area appeared to be sufficiently large to average the mechanical fluctuations of the surface, resulting in more representative hardness and modulus values. It is not that important whether the center of an indent is focused on a grain or an interfacial region.

Overall, the SEM micrographs corroborate the results shown in Figs. 2–4. Nevertheless, it is unclear if the critical contact areas of 20 and 40 μm mentioned above are simply correlated with the grain size shown in Fig. 5. This might be because there are other sources of structural inhomogeneity. For example, compaction causes structural damage inside the primary particle, which serve as the source of mechanical property fluctuations. Furthermore, a primary particle is usually not a single crystal, and before compaction, is a complex structure of grains and grain boundaries. The micro-indentation results will respond all the sources of structural inhomogeneity.

3.4 AFM investigation

There are spatial fluctuations in the mechanical properties on a much finer scale. Besides the spatial fluctuation on the

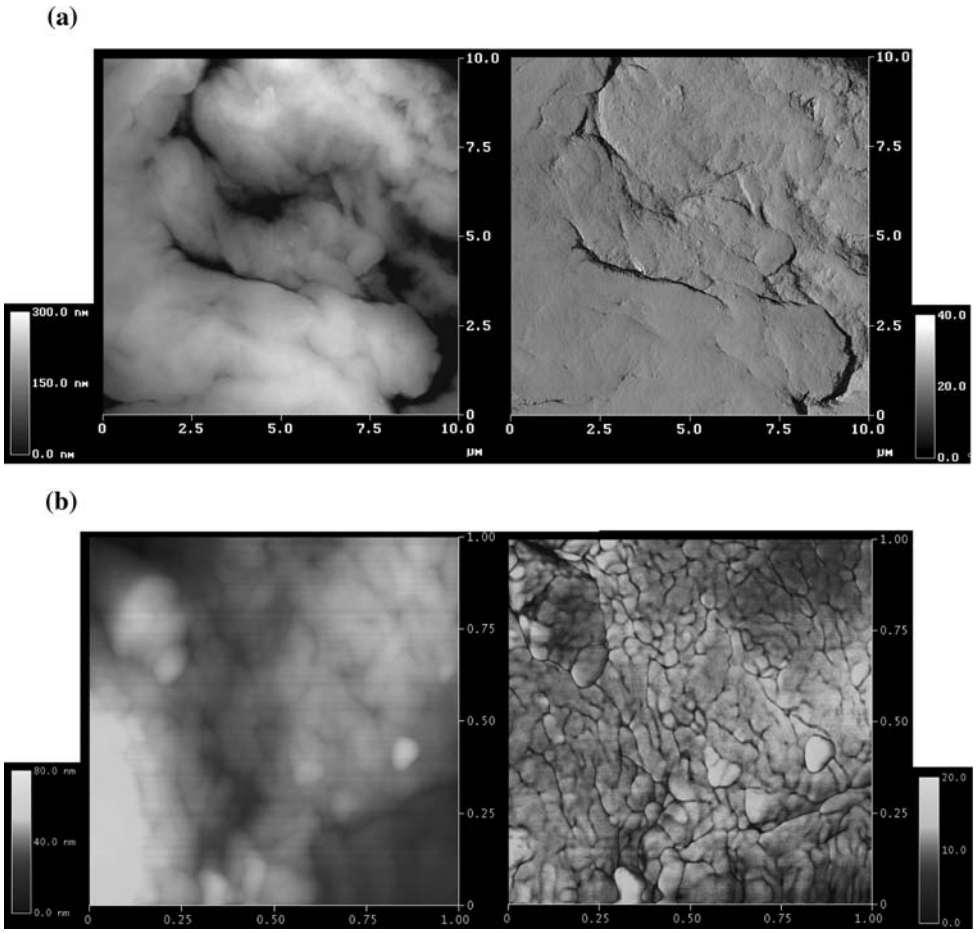

Fig. 6 AFM height (left) and phase (right) images of microcrystalline cellulose compact surface. The widths of micrographs are 10 × 10 (**a**) and 1 × 1 (**b**) μm. (rectangular plate samples) Asp = set-point amplitude, Ao = amplitude of driving oscillation. (**a**) Asp = 2,352 mV, Asp/Ao = 0.34 (**b**) Asp = 2,352 mV, Asp/Ao = 0.72

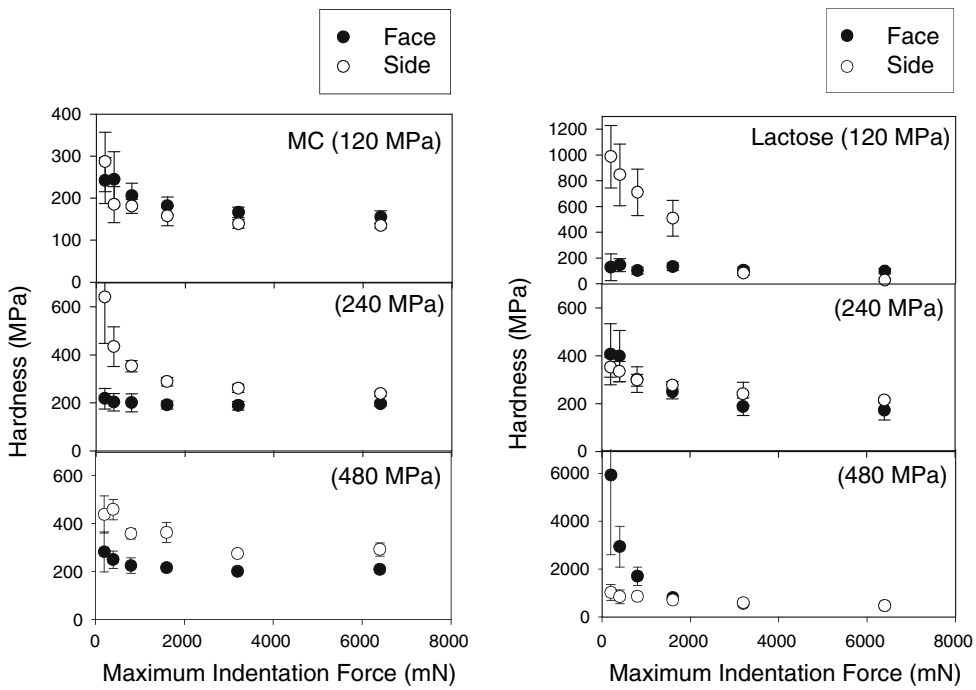

Fig. 7 Indentation hardness of microcrystalline cellulose (left) and lactose (right) compacts as a function of maximum force of indentation. The compaction pressure varies from 120 to 480 MPa. (disk samples) (**a**) MC, face surface (**b**) MC, side surface (**c**) Lactose, face surface (**d**) Lactose, side surface

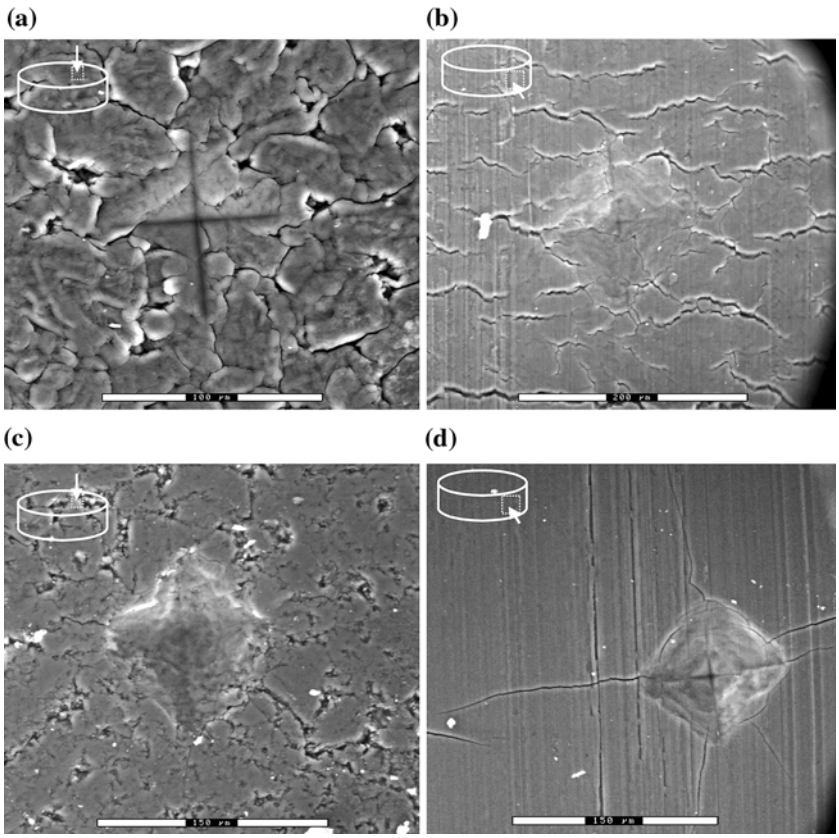

Fig. 8 ESEM micrographs of indents (3,200 mN maximum indentation force) on compacts: (**a**) face surface of microcrystalline cellulose; (**b**) side surface of microcrystalline cellulose; (**c**) face surface of lactose; (**d**) side surface of lactose. (disk samples)

micron scale shown in Fig. 5, fluctuations on the nanometer scale should exist and can be examined using AFM indentation techniques [25, 26].

AFM imaging in tapping mode showed that the actual indentation of the AFM tip into the specimen surface is possible by changing the A_{sp}/A_o ratio (A_o: free oscillation amplitude (amplitude of driving oscillation), A_{sp}: set-point amplitude) [27–29]. A decrease in A_{sp}/A_o ratio results in more penetration. As the AFM tip penetrates the surface, its phase images reveal the distribution of its mechanical properties in the 2D images [29]. On the other hand, the height images are less sensitive to fluctuation in the surface mechanical properties.

Figure 6 shows the results of tapping mode AFM of the MC compacts. Figure 6a shows the distribution of the mechanical strength on the micron scale, where a few line structures are visible. These line structures might be shear deformation lines or simply microcracks, and may have relatively low indentation resistance. The height image (Fig. 6a left) also shows similar features. The line structures appear to be sufficiently distinct to appear in both images. As magnification increases, smaller features become noticeable. Figure 6b shows the grain structures of the 50–200 nm domains. Their boundaries appear to be relatively weak against indentation. The grain structures might be intrinsic semicrystalline domains inside MC particles. They are more distinct in the phase images at an optimum A_{sp}/A_o ratio than in the height images. Indentation too deep or too shallow prevents the grain structures from being observed. Structural inhomogeneity on a scale smaller than tens of microns will contribute the increase in the standard deviation of the hardness values with a decreasing in MIF. However, a quantitative detailed correlation between the AFM and the micro-indentation results was difficult to establish.

3.5 Anisotropy related issues of compacts

Compaction itself induces inhomogeneity in a compact. Micro-indentation can reveal the nature of compaction-induced inhomogeneity by probing different regions of the compacts. Complete 3D mapping of the indentation hardness is possible by probing all the surface area of a compact [10].

Instead of the tedious tests of complete mapping, rather simple micro-indentation testing can reveal the useful characteristics of inhomogeneity. A unique understanding came from the comparison between the face and side surfaces of a compact. In a disk-shape tablet, the compaction pressure acts perpendicular to its face surface and parallel to its side surface. Densification progresses mainly along

the direction of the compaction pressure. A series of micro-indentation results on the face and side surfaces of a compact provides complicated but interesting behavior (Fig. 7). First of all, the indentation hardness values and their standard deviations generally increase with decreasing MIF. (Although the specimen geometry and compaction forces are different, the general trends shown in Figs. 2–4 can also be observed in Fig. 7.)

The effect of the compaction pressure can be examined by comparing the indentation hardness values of a high MIF (>1,600 mN). (The indentation hardness of a low MIF is complicated by the inhomogeneity of the granular structures.) Like the conventional generalization, hardness generally increases as compaction pressure increases [10]. In detail, the hardness of the MC side surface was similar to that of its face surface at 120 MPa, and then increased further with increasing compaction pressure. At 480 MPa, the hardness values of the side surface were distinctly higher than those of the face surface. On the other hand, the hardness of the LT side surface did not show a strong increase with increasing compaction pressure. The opposite trend can be found at a low MIF: The hardness of the face surface appears to increase more with increasing compaction pressure than that of the side surface.

The difference in the compaction pressure dependence might be explained by the differences in the material properties. Compaction progresses via various micro-mechanical deformations. In the cases of ductile semi-crystalline polymer particles such as MC, densification progresses mainly by significant plastic deformation, while it progresses more through microcracking in the brittle crystalline LT [1, 10]. Microcracking densification is less efficient in increasing indentation hardness than the other. A corollary is that densification will more effectively strengthen the side surface of the MC than that of LT. The face surface of a compact is perpendicular to the compaction pressure, and its hardness might be less dependent on the compaction pressure. Therefore, the compaction pressure dependence of the indentation hardness can depend on the mechanical properties of the material.

By comparing the indents left on the surfaces, the differences in micro-mechanical processes can be traced. Figure 8a, b, and c show the interstitial gaps (grain boundaries) generated during compaction, largely between primary particles. In Fig. 8d, micro-indentation on the side surface of the LT produced a distinct microcracking phenomenon. On the other hand, significant microcracking was not induced by micro-indentation on the other surfaces. This result is consistent with those shown in Fig. 7.

The size of the cracks in Fig. 8d provides important information. They were not too small to observe nor too large to destroy the integrity of the compact. The size of a crack indicates material resistance to fracture. The fracture toughness, which is an important parameter related to capping, delaminating, etc, can be calculated by measuring the crack size [2, 7]. The average stress intensity factor of all the LT specimens was 0.10 ± 0.04 MPa-m$^{1/2}$. In a previous report, lactose had stress intensity factor values between 0 and 0.4 MPa-m$^{1/2}$ depending on porosity and other materials parameters [12, 13, 30]. The relatively low value is reasonable because only the side surfaces, which are more susceptible to cracking (so more important) were probed. The inhomogeneity information of the fracture related properties can also be obtained using this technique.

4 Discussion

Porous pharmaceutical compacts have grain structures like ceramics. The grain structures of pharmaceutical compacts could be even more complex than ceramics because they often have particles of a wide range of different physical properties. Therefore, the indentation process in pharmaceutical compacts is more difficult to define. During indentation, considerable compaction often occurs as a result of grain-boundary fracture and grain rearrangement. In a typical indentation test on porous materials, a semi-log plot of the hardness versus the log of the pressure used to form a porous specimen is linear, which suggests that the hardness of a porous body can be estimated from the value of the compaction pressure [10, 19].

The indentation hardness was found to generally increase with decreasing MIF. A widely accepted explanation in materials science is from strain gradient plasticity theory [23, 24]. The square of the plastic flow stress is linearly dependent on the strain gradient. As the size of the indents decreases, more strain gradient develops and more strain hardening follows. Indentation generates grain boundaries. The blocking of dislocation by grain boundaries accompanies a decrease in the relative grain size resulting in an increase in hardness. Regarding this effect, there have been several equations proposed for ceramic materials, but they do not appear to be readily adaptable to pharmaceutical materials with poorly defined internal structures [23, 24].

Besides the strain gradient effect, friction between the indenter and material surface can be a reason for the effects of the MIF [31]. The top surface region could be stronger than the other regions, because it can harden during compaction [10]. Thus, as the size of the indents decreases, it is possible that the indenter probes only the hardened top surface regions. Additionally surface adsorption and chemisorption can also influence the effect of the MIF.

Although the effects of the strain gradient have been established in ceramic materials, it is not straightforward to

apply this concept to pharmaceutical compacts [23, 24]. Instead, the standard deviation of the indentation hardness can indicate the homogeneity of compacts. In particular, a simple micro-indentation test on the side and face surfaces of the compacts with changing MIF was found to be a useful technique for revealing the structural inhomogeneity of the compacts. The materials response to densification, fracture resistance, grain structures and sizes can be assessed simultaneously using this test.

Among the indentation tests in all scales, the micro-indentation seems to be in the proper size range for conventional pharmaceutical compacts. The indentation area of the micro-indentation is generally too small to assess the average indentation hardness, but too large to map the distribution of the hardness in a compact. However, it is convenient to probe the structural inhomogeneity of compacts since it is small enough to have the influence of the inhomogeneity and large enough to perform conveniently without problems with instrumentation, which is often associated with the sensitive nano-indentation.

The results of the microscopy investigation were used to corroborate the micro-indentation results, but they do not necessarily correspond to each other. Mechanical properties probed by micro-indentation can be different from the topological maps obtained from SEM. The edges of granular structures and microcracks are distinct in both the tests and serve as the links between them. AFM can provide information on the qualitative 2D distribution of the indentation resistance [27–29].

The structural inhomogeneity should eventually be related to the final physical and chemical properties of the compact. For example, the structural inhomogeneity reflects microcracking and grain boundary formation due to compaction, as shown in Fig. 7. The susceptibility of the tablet to chipping, delamination, etc, would depend on the scattering of mechanically weak regions as well as to the extent of their weakness. The relatively convenient micro-indentation characterization technique offers a way of approaching complex tablet problems.

5 Conclusions

Micro-indentation tests could measure the indentation hardness and modulus of compacts. However, as the MIF decreased, the results showed the effect of different influences such as strain gradient effects. An analysis of these influences does not appear to be straightforward. Nevertheless, variations in the standard deviation of the indentation hardness and modulus as a function of the MIF did reveal micro-structural information of the compacts. The lactose and microcrystalline cellulose compacts showed the significant development of inhomogeneity below 800 mN MIF. The level of structural inhomogeneity increased with decreasing MIF, and the SEM and AFM micrographs reflected the indentation results. A complex dependence on compaction pressure was also shown. The application of micro-indentation to the face and side surfaces of the compacts can provide more information of the structural inhomogeneity associated with the anisotropy that develops as a result of compaction.

Acknowledgements I like to thanks Dr. Batra, Dr. Bika and Dr. Panmai at Merck for their help for JL to start working on this testing. This work was supported by Korea Energy Management Corporation (KEMCO) (Project #: 2006-E-ID11-P-30–3-020).

References

1. H. E. Boyer, “Hardness testing” (ASM International, 1994)
2. W. C. DUNCAN-HEWITT and G. C. WEATHERLY, *J. Mater. Sci. Lett.* **8** (1989) 1350
3. W. C. DUNCAN-HEWITT and G. C. WEATHERLY, *Pharm. Res.* **6** (1989) 1060
4. W. C. DUNCAN-HEWITT and G. C. WEATHERLY, *Pharm. Res.* **6** (1989) 373
5. M. CELIK and M. E. AULTON, *Drug Development and Industrial Pharmacy*. **22**(1) (1996) 67
6. S. K. LUM and W. C. DUNCAN-HEWITT, *Pharm. Res.* **13** (1996) 1739
7. K. V. PRASAD, D. B. SHEEN and J. N. SHERWOOD, *Pharm. Res.* **18** (2001) 867
8. R. KUPPUSWAMY, S. R. ANDERSON, L. L. AUGSBURGER and S. W. HOAG, *AAPS Pharmsci.* **3** (2001) 1
9. J. T. Carstensen, “Advanced pharmaceutical solids” (Marcel Dekker, 2001 p. 387, p. 407)
10. G. Alderborn and C. Nystrom, “Pharmaceutical powder compaction technology” (Marcel Dekker, 1996)
11. X. LIAO and T. S. WIEDMANN, *J. Pharm. Sci.* **94** (2005) 79
12. R. J. ROBERTS, R. C. ROWE and P. YORK, *Pharm. Sci.* **1** (1995) 501
13. R. J. ROBERTS, R. C. ROWE and P. YORK, *Int. J. Pharm.* **125** (1995) 157
14. J. LEE, *J. Pharm. Sci.* **92** (2003) 2057
15. W. C. DUNCAN-HEWITT, *Powder Technol.* **60** (1990) 265
16. W. C. DUNCAN-HEWITT, *Drug Dev. Ind. Phar.* **19**(17&18) (1993) 2197
17. W. C. DUNCAN-HEWITT and G. C. WEATHERLY, *J. Pharm. Sci.* **79** (1990) 147
18. W. C. DUNCAN-HEWITT and G. C. WEATHERLY, *J. Pharm. Sci.* **79** (1990) 273
19. M.-C. LIN and W. C. DUNCAN-HEWITT, *Int. J. Pharm.* **106** (1994) 187
20. N. X. RANDALL, C. JULIA-SCHNUTZ, J. M. SORO, J. von STEBUT and G. ZACHARIE, *Thin Solid Films.* **308–309** (1997) 297
21. W. C. OLIVER and G. M. PHARR, *J. Mater. Res.* **7** (1992) 1564
22. G. M. PHARR, W. C. OLIVER and F. R. BROTZEN, *J. Mater. Res.* **7** (1992) 613
23. H. GAO, Y. HUANG, W. D. Nix and J. W. HUTCHINSON, *J. Mech. Phys. Solids.* **47** (1999) 1239
24. N. A. FLECK and J. W. Hutchinson, *J. Mech. Phys. Solids.* **41** (1993) 1825
25. J. LEE, *J. Phar. Sci.* **93** (2004) 2310
26. J. LEE, *Macromol. Biosci.* **5** (2005) 1085

27. G. BAR, M. GANTER, R. BRANDSCH, L. DELINEAU and M.-H. WHANGBO, *Langmuir* **16** (2000) 5702
28. S. N. MAGONOV, V. ELINGS and M.-H. WHANGBO, *Surface Science.* **375** (1997) L385
29. N. Z. QURESHI, M. ROGUNOVA, E. V. STEPANOV, G. CAPACCIO, A. HILTNER and E. BAER, *Macromolecules* **34** (2001) 3007
30. R. J. ROBERTS, R. C. ROWE and P. YORK, *Int. J. Pharm.* **91** (1993) 173
31. R. VAIDYANATHAN, M. DAO, G. RAVICHANDRAN and S. SURESH, *Acta Mater.* **49** (2001) 3781